PLOS | ONE

RESEARCH ARTICLE

Warming Amplification of Minimum and Maximum Temperatures over High-Elevation Regions across the Globe

Xiaohui Fan[1☯], Qixiang Wang[1☯], Mengben Wang[1]*, Claudia Villarroel Jiménez[2]

1 Institute of Loess Plateau, Shanxi University, Taiyuan, Shanxi Province, China, **2** Dirección Meteorológica de Chile, Santiago, Chile

☯ These authors contributed equally to this work.
* mbwang@sxu.edu.cn

Citation: Fan X, Wang Q, Wang M, Jiménez CV (2015) Warming Amplification of Minimum and Maximum Temperatures over High-Elevation Regions across the Globe. PLoS ONE 10(10): e0140213. doi:10.1371/journal.pone.0140213

Editor: Inés Álvarez, University of Vigo, SPAIN

Received: May 21, 2015

Accepted: September 23, 2015

Published: October 13, 2015

Data Availability Statement: All relevant data are within the paper.

Funding: This work was supported by the Natural Science Foundation of Shanxi Province for Young Scholars (China) (2013021030-2), the Project for Key and Special Subjects of Shanxi Province (China) and the Innovative Project for Excellent Graduate Students of Shanxi Province (China). The funders had no role in study design, data collection and analysis, decision to publish, or preparation of the manuscript.

Competing Interests: The authors have declared that no competing interests exist.

Abstract

An analysis of the annual mean temperature (T_{MEAN}) (1961–2010) has revealed that warming amplification (altitudinal amplification and regional amplification) is a common feature of major high-elevation regions across the globe against the background of global warming since the mid-20th century. In this study, the authors further examine whether this holds for annual mean minimum temperature (T_{MIN}) and annual mean maximum temperature (T_{MAX}) (1961–2010) on a global scale. The extraction method of warming component of altitude, and the paired region comparison method were used in this study. Results show that a significant altitudinal amplification trend in T_{MIN} (T_{MAX}) is detected in all (four) of the six high-elevation regions tested, and the average magnitude of altitudinal amplification trend for T_{MIN} (T_{MAX}) [0.306±0.086 °C km^{-1}(0.154±0.213 °C km^{-1})] is substantially larger (smaller) than T_{MEAN} (0.230±0.073 °C km^{-1}) during the period 1961–2010. For the five paired high- and low-elevation regions available, regional amplification is detected in the four high-elevation regions for T_{MIN} and T_{MAX} (respectively or as a whole). Qualitatively, highly (largely) consistent results are observed for T_{MIN} (T_{MAX}) compared with those for T_{MEAN}.

Introduction

Two key questions related to climate changes in high-elevation regions are whether elevation-dependent warming commonly occurs in these regions, and whether high-elevation regions are warming faster than their low-elevation counterparts [1–5]. During the recent decades, numerous studies have focused on the first issue based on surface observations. Although most studies focused on the mean temperature [6–11], a few other studies also analyzed the minimum temperature and maximum temperature [11–15]. However, the elevation dependency was statistically confirmed only for the minimum temperature anomalies (1979–1993) in the Swiss Alps[12]. On the second issue, Falvey and Garreaud [16] used daily mean temperature series (1979–2006) and identified a strong contrast between surface cooling at low-lying (coastal) stations and warming in the Andes in central and northern Chile. Additionally,

greater warming was observed at high-elevation sites than at low-lying sites in the Swiss Alps based on the trends in maximum and minimum temperatures [17–18].

In the latest study, based on a dataset of annual mean temperature (T_{MEAN}) series (1961–2010) from 2367 stations around the world, Wang *et al.* [19] revealed that warming amplification (altitudinal amplification and regional amplification) is a common feature of major high-elevation regions across the globe against the background of global warming since the mid-20th century. These authors reached this conclusion by developing the altitudinal warming component extraction equation (AWCE equation), and employing the paired region comparison method. In this study, we further examine whether this holds for annual mean minimum temperature (T_{MIN}) and annual mean maximum temperature (T_{MAX}).

Materials and Methods

2.1 Data

This study used a dataset of 1,494 T_{MIN} and 1,448 T_{MAX} station series (1961–2010) around the world (Fig 1). Of all the stations, 1334 are the same stations, representing 89.3% (92.1%) of the total T_{MIN} (T_{MAX}) stations, and 652 (641) T_{MIN} (T_{MAX}) stations are sited at the six high-elevation regions tested (Fig 2), of which 636 are the same stations, representing 97.5% (99.2%) of the total high-elevation region T_{MIN} (T_{MAX}) stations.

The data were compiled from 6 sources: the Global Historical Climatology Network Monthly (GHCNM) version 3.2.0dataset [20]; the National Meteorological Information Center of China (NMICC); MeteoSwiss; the Latin American Climate Assessment and dataset (LACAD)[21]; the European Climate Assessment & Dataset (ECA&D)[22]; and the National Weather Service of Chile (NWSC). The data for the GHCNM, NMICC, ECA&D and NWSC were available for the entire period 1961–2010, while the data for the LACAD were available for the period 1961–2006.

To obtain the annual time series from the daily minimum and maximum temperatures from the ECA&D and NWSC, two steps (or two criteria) were required. A monthly mean value was first calculated for the available days if no more than 3 days of data were missing in that month; then, an annual mean value was computed from the monthly means if 12 monthly values were present in that year. For the monthly data from other sources, the annual time series was calculated using the second criterion. After the establishment of the T_{MIN} and T_{MAX} series (1961–2010), the series that had at least37yearsof complete data (i.e., 12 months per year) were selected for homogeneity testing using RHtests V3 [23]. The series that had obvious inhomogeneity were excluded. However, the series from the LACAD with at least 30 years of complete data were also included in the homogeneity test because the source dataset ended in 2006, the available stations in the Andes were very sparse, and no other data are available at present. The final dataset consisted of 909 (874), 459 (459), 58 (53), 36 (33),17 (17) and 15 (12)T_{MIN}(T_{MAX}) stations from the GHCNM; NMICC, MeteoSwiss, LACAD, ECA&D and NWSC, respectively, with 37, 41, 37, 30, 41and 40yearsof complete data, respectively.

2.2 Methods

2.2.1 Test of temperature trend. The trend for a station (or a region as a whole) was extracted from the anomalies (relative to the 1961–1990 mean) using the Mann-Kendall method [24–25]. The trend slope was estimated using Sen's method [26] and the trend significance was determined using the Mann-Kendall test [24–25] with an iterative procedure [27].

2.2.2 Test of altitudinal amplification. The methodology for evaluation of the altitudinal amplification trend for T_{MIN} (T_{MAX}) within a high-elevation region was exactly the same as for T_{MEAN} in the previous study [19], consisting of the following four steps:

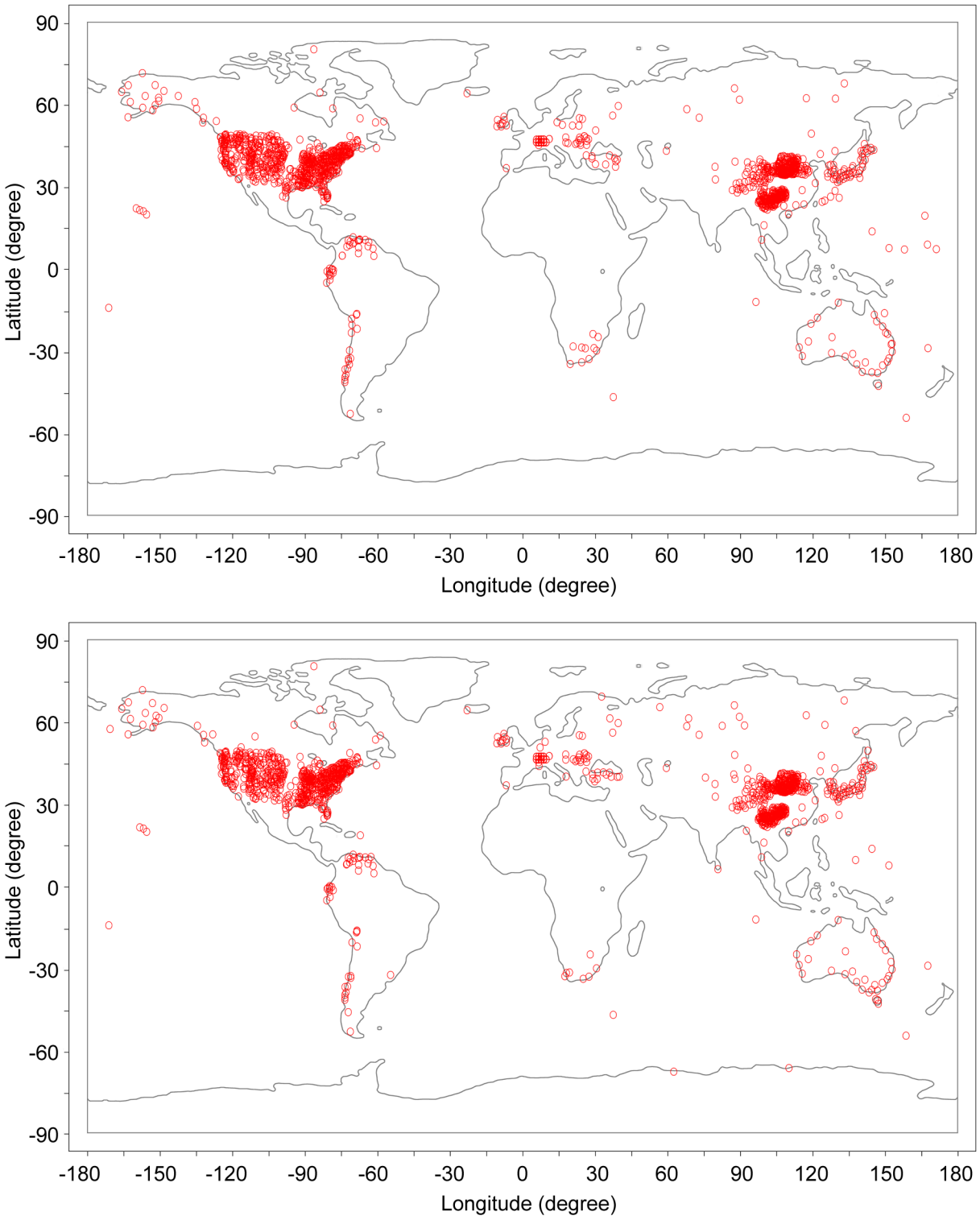

Fig 1. Distribution of 1494 stations with annual mean minimum temperature series (top) and 1448 stations with annual mean maximum temperature series (bottom) used for this study around the globe. The boundaries of continents, generated with the Adobe Photoshop CS6, are not necessarily identical to the original image, and are therefore for illustrative purpose only.

doi:10.1371/journal.pone.0140213.g001

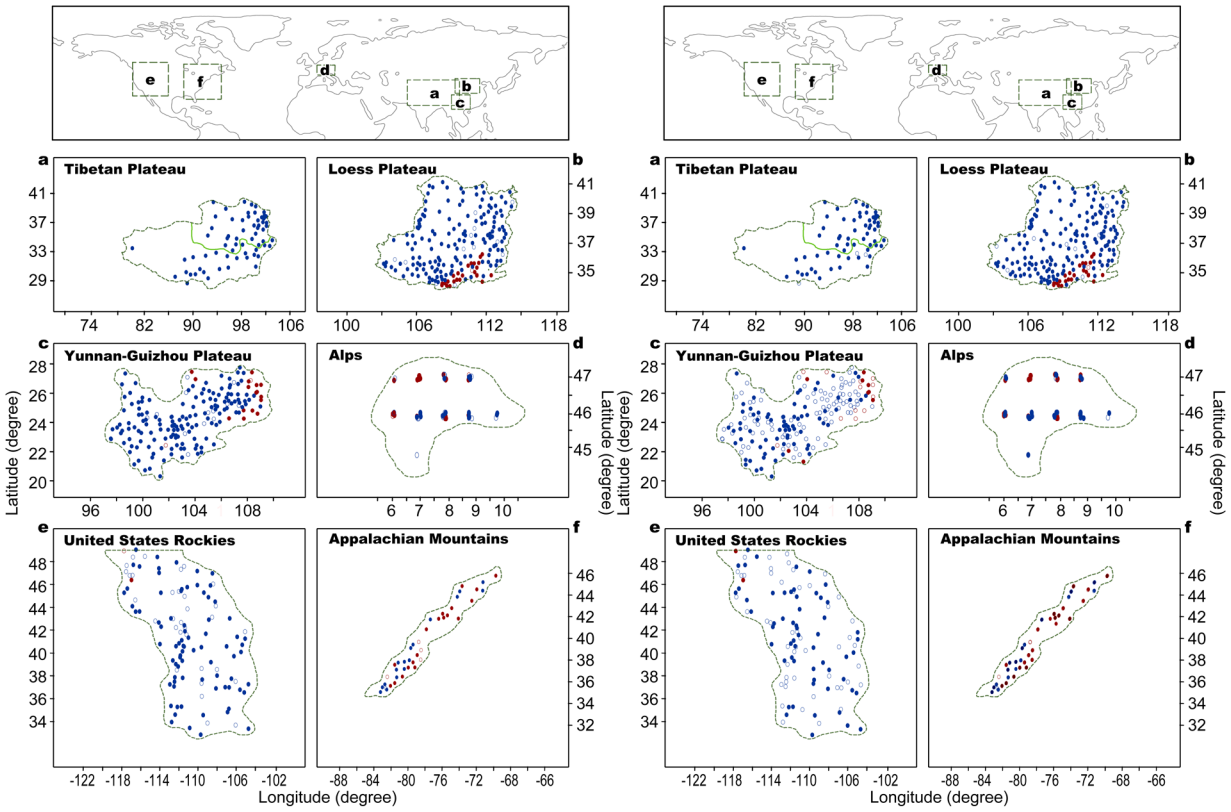

Fig 2. Distribution of stations in the high-elevation regions. The left panels show the stations with annual mean minimum temperature series, and the right panels show the stations with annual mean maximum temperature series. The high-elevation stations at ≥500m asl, and ≥200m to <500 m asl are shown in blue and red colors, respectively. Dots and circles stand for significant and non-significant positive trends, respectively. The boundaries of continents and the high-elevation regions, generated with the Adobe Photoshop CS6, are for illustrative purpose only.

doi:10.1371/journal.pone.0140213.g002

1. Transformation of altitude (in meter), latitude (in degree) and longitude (in degree) into *ALT*, *LAT* and *LONG* (all in km) for each station using the following equations,

$$ALT = altitude/1000, \quad (1)$$

$$LAT = latitude \times 111.317, \quad (2)$$

$$LONG = longitude \times \pi \times R \times \cos(latitude)/180. \quad (3)$$

where 111.317 (expressed in km) is the distance constant per degree of latitude, and *R* is the radius of the Earth. Because the distance between two degrees of longitude changes with latitude, eq (3) is necessary.

2. Estimation of the effect coefficients of altitude, latitude and longitude (EC_{ALT}, EC_{LAT} and EC_{LONG}, respectively) on a regional scale using stepwise regression. This procedure was performed with the model of fit $y = b_1x_1 + b_2x_2 + b_3x_3 + c$, where the long-term (1961–2010) average T_{MIN} and T_{MAX} values ($\boldsymbol{T_{AVG}}$ in general, °C) and the *ALT*, *LAT* and *LONG* values of the individual stations within a region were taken as the dependent (y) and independent variables (x_1, x_2, and x_3), respectively. The negative values of the regression coefficients (b_1, b_2 andb_3) estimated for *ALT*, *LAT* and *LONG* (i.e., the temperature lapse rates along the altitudinal, latitudinal and longitudinal gradients) were taken as EC_{ALT}, EC_{LAT} and EC_{LONG},

respectively. When an independent variable was not introduced (i.e., the partial correlation coefficient for it was not significant at the 0.05 level), its effect coefficient was considered to be zero.

3. Extraction of the warming component of altitude (Q_{ALT}) from the station warming rate (Q_{TOTAL}) for each station within a high-elevation region using the following equation,

$$Q_{ALT} = \frac{Q_{TOTAL} \times EC_{ALT} \times ALT}{\sqrt{(EC_{ALT} \times ALT)^2 + (EC_{LAT} \times LAT)^2 + (EC_{LONG} \times LONG)^2}}. \quad (4)$$

where Q_{TOTAL} in T_{MIN} and T_{MAX} is expressed in °C 50-yrs^{-1}, and *ALT*, *LAT* and *LONG* are all expressed in km for each station, and EC_{ALT}, EC_{LAT} and EC_{LONG} are constant values for every station within the region, and are expressed in °C km^{-1}. The result, Q_{ALT}, is also expressed in °C 50-yrs^{-1}.

4. Test of the altitudinal amplification trend for each region. Based on the Q_{ALT} values extracted from the individual stations, the altitudinal amplification trend was evaluated by regressing Q_{ALT} against *ALT* to obtain the amplification factor (Q_{ALTAMP}, in °C km^{-1}50-yrs^{-1}) over the period 1961–2010.

Besides, if assuming that the temperature change in a high-elevation region is predominately controlled by altitude and latitude, then the EC_{ALT}, and EC_{LAT} will be estimated using the model of fit $y = b_1x_1 + b_2x_2 + c$, where the long-term average T_{MEAN} (T_{MIN} or T_{MAX}; in °C), and the *ALT* and *LAT* at individual stations within the region will be used as the dependent (y) and independent variables (x_1 and x_2), respectively. The negative values of b_1 and b_2 will be taken as the EC_{ALT} and EC_{LAT}, respectively. The extraction of Q_{ALT} from Q_{TOTAL} for each station is conducted either using eq (4), where the EC_{LONG} is assumed to be zero, or using the following equation:

$$Q_{ALT} = \frac{Q_{TOTAL} \times EC_{ALT} \times ALT}{\sqrt{(EC_{ALT} \times ALT)^2 + (EC_{LAT} \times LAT)^2}}. \quad (5)$$

Furthermore, if assuming that the temperature change in a high-elevation region is only controlled by altitude (both EC_{LAT} and EC_{LONG} are considered to be zero), Q_{ALT} will be equal to Q_{TOTAL},

$$Q_{ALT} = \frac{Q_{TOTAL} \times EC_{ALT} \times ALT}{\sqrt{(EC_{ALT} \times ALT)^2}} = \frac{Q_{TOTAL} \times EC_{ALT} \times ALT}{EC_{ALT} \times ALT} = Q_{TOTAL}. \quad (6)$$

It is clear that this equation is a special case of eq (4) or eq (5).

2.2.3 Test of regional amplification. The regional amplification was tested using the paired-region comparison method [19]. Each of the paired high and lower elevation regions were selected using a method similar to the belt transect method. Each paired regions are located at the same latitudes, and has the equal longitude range. The sampled area is a northeast-southwest parallelogram for the Appalachian Mountains, and its west low-lying counterpart (Table 1).

However, the regional amplification was not only evaluated for T_{MIN} and T_{MAX} as for T_{MEAN} [19], but also for T_{MIN} and T_{MAX} as a whole. (1) The regional amplification was evaluated for T_{MIN} and T_{MAX} separately when a similar asymmetric warming in T_{MIN} and T_{MAX} occurs between one paired regions; that is, the magnitude of the trend is greater for T_{MIN} than T_{MAX} (or for T_{MAX} than T_{MIN}) in both high- and low-elevation regions. (2) The regional

Table 1. The latitudes, longitudes, and average altitudes of the paired regions across the globe.

No.	Paired regions	Latitude	Longitude	Avg alt (km)	n
		Annual mean minimum temperature			
1a	North Tibetan Plateau	34–38°N	93–102°E	3.1365	23
1b	Loess Plateau	34–38°N	103–112°E	1.0173	112
2a	East Loess Plateau	34–38°N	107–112°E	0.8036	83
2b	North China Plain	34–38°N	114–119°E	0.0782	17
3a	Alps	45–48.5°N	5.5–16.5°E	0.9598	58
3b	East lower region	45–48.5°N	17°E–28°E	0.2681	17
4a	Southeast Rockies (USA)	36–41°N	104–109°W	2.0804	17
4b	East lower region	36–41°N	86–91°W	0.1793	53
5a	Appalachian Mountains	35–46°N	68.5–72.6°W at 46°N 81.7–85.8°W at 35°N	0.4757	56
5b	West lower region	35–46°N	73–77.1°W at 46°N 86.2–90.3°W at 35°N	0.2593	66
		Annual mean maximum temperature			
1a	North Tibetan Plateau	34–38°N	93–102°E	3.1365	23
1b	Loess Plateau	34–38°N	103–112°E	1.0452	118
2a	East Loess Plateau	34–38°N	107–112°E	0.8044	85
2b	North China Plain	34–38°N	114–119°E	0.0782	17
3a	Alps	45–48.5°N	5.5–16.5°E	0.9905	53
3b	East lower region	45–48.5°N	17°E–28°E	0.2681	17
4a	Southeast Rockies (USA)	36–41°N	104–109°W	2.0747	17
4b	East lower region	36–41°N	86–91°W	0.1764	54
5a	Appalachian Mountains	35–46°N	68.5–72.6°W at 46°N 81.7–85.8°W at 35°N	0.4759	54
5b	West lower region	35–46°N	73–77.1°W at 46°N 86.2–90.3°W at 35°N	0.2546	66

doi:10.1371/journal.pone.0140213.t001

amplification was evaluated for T_{MIN} and T_{MAX} as a whole (the average magnitude of T_{MIN} and T_{MAX} trends was used for comparison) when an opposite asymmetric warming in T_{MIN} and T_{MAX} occurs between one paired regions; that is, the magnitude of the trend is greater for T_{MIN} than T_{MAX} in one region, whereas the magnitude of the trend is greater for T_{MAX} than T_{MIN} in its counterpart. In this situation, the separate analysis of regional amplification for T_{MIN} and T_{MAX} would not only make the difference in T_{MIN} or T_{MAX} (or both) appear very large between the paired regions, but would also make the warming in T_{MIN} or T_{MAX} look even weaker at times for the high-elevation region than its lower counterpart, and vice versa, even if the average warming (the magnitude of the T_{MEAN} trend) is greater in the high-elevation region than its lower counterpart.

Results

3.1 Altitudinal amplification

Figs 3 and 4 depict the relationship between the altitudinal warming components (Q_{ALT}s) and station altitudes within each high-elevation region for T_{MIN} and T_{MAX}, respectively. A significant altitude amplification trend in T_{MIN} is detected in all the high-elevation regions tested (the Tibetan Plateau, Loess Plateau, Yunnan-Guizhou Plateau, Alps, US Rocky Mountains, and Appalachian Mountains), whereas a significant or a marginally significant altitude amplification trend in T_{MAX} is observed in four of the high-elevation regions (significant: the Yunnan-

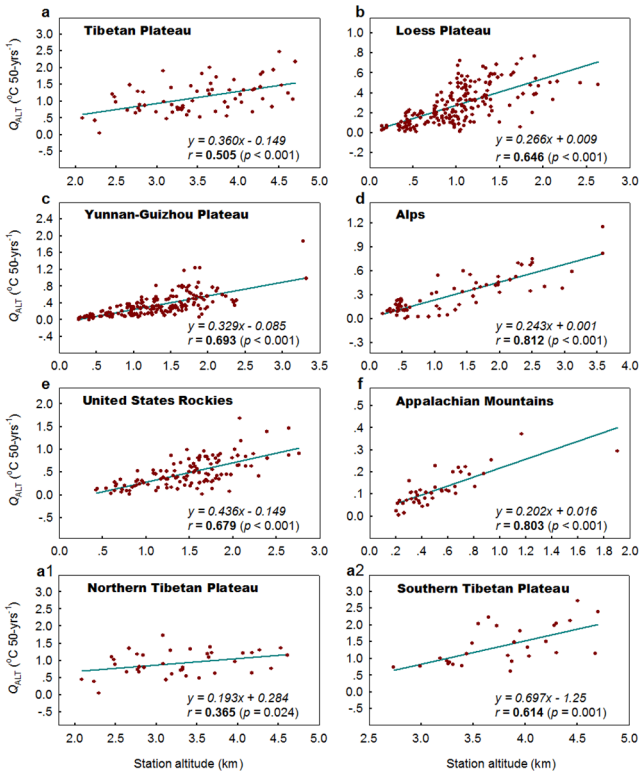

Fig 3. Relationship between altitudinal warming components (Q_{ALT}s) of annual mean minimum temperature and station altitudes for the high-elevation regions across the globe. Dots represent Q_{ALT}s, and dark cyan lines indicate linear regression lines. The magnitude of altitudinal amplification trend (Q_{ALTAMP}, the gradient of the regression line) is expressed in °C km^{-1}50-yrs^{-1}. Pearson correlation coefficients (*r*) are shown with two-tailed *p* values in parentheses. Significant coefficients (at the 0.05 level) are set in bold.

doi:10.1371/journal.pone.0140213.g003

Guizhou Plateau, Alps, and Appalachian Mountains; marginally significant: the Tibetan Plateau). No altitudinal amplification in T_{MAX} is detected in the Loess Plateau, and US Rocky Mountains.

In the regions where altitudinal amplification trends have been confirmed for T_{MIN} and T_{MAX}, the magnitudes of the amplification trends are generally greater for T_{MIN} than for T_{MAX} (Table 2). If the magnitude of the altitudinal amplification trend is taken as zero when no altitudinal amplification trend is detected, the average magnitude of altitudinal amplification trends for the six regions is 0.306 ± 0.086 °C km^{-1} 50-yrs^{-1} and 0.154 ± 0.213 °C km^{-1} 50-yrs^{-1} for T_{MIN} and T_{MAX}, respectively. This indicates a remarkable asymmetry in the altitudinal amplification between T_{MIN} and T_{MAX}. The average magnitude of amplification trends is 0.33 times greater for T_{MIN} but 0.33 times smaller for T_{MAX} compared with the magnitude for T_{MEAN} (0.230 ± 0.073 °C km^{-1}) during the period 1961–2010.

Similar results are obtained (Table 3) provided that temperature change in high-elevation regions is predominately controlled by two variables (altitude and latitude) rather than three variables (altitude, latitude and longitude). The average magnitude of the altitudinal amplification trends for the six regions is0.300 ±0.089 °C km^{-1}50-yrs^{-1} and 0.155±0.212 °C km^{-1} 50-yrs^{-1}for T_{MIN} and T_{MAX}, respectively;0.32 times greater for T_{MIN} but 0.32 times smaller for T_{MAX} compared with that (0.228 ±0.069 °C km^{-1}) for T_{MEAN} during the same period. This indicates

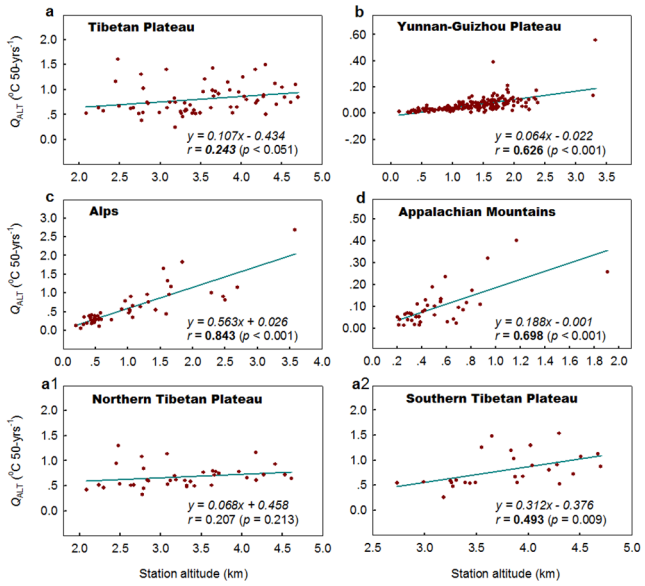

Fig 4. Same as Fig 3 but for annual mean maximum temperature, with the marginally significant coefficient (at the 0.10 level) in italic bold.

doi:10.1371/journal.pone.0140213.g004

that the longitude effect, though significant in three of the regions tested, is almost negligible in quantifying the altitudinal amplification trends in high-elevation regions.

However, if assuming that temperature change in high-elevation regions is only controlled by altitude, contrasting results are obtained for T_{MEAN}[19], T_{MIN} and T_{MAX}(Table 4). The differing results for T_{MEAN}, T_{MIN} and T_{MAX} among the high-elevation regions could be attributed to the difference in signal intensity of the Q_{TOTAL} values[28] and the region-specific interactions between altitude and latitude [19]in the individual regions (see the 'Discussion'section for details).

3.2 Regional amplification

Figs 5 and 6 depict the monotonic trends (1961–2010) in the paired regions for T_{MIN} and T_{MAX}, respectively. Among the five paired regions, the magnitude of the T_{MAX} trend is larger than the T_{MIN} trend for the Alps and its low-lying counterpart, whereas the magnitude of the T_{MIN} trend is larger than the T_{MAX} trend for the Appalachian Mountains and its low-lying counterpart. Despite this difference between these two paired regions, similar asymmetric warming is detected in each paired regions. It is clear that greater warming is only observed in T_{MIN} for the Alps than its east low-lying counterpart, whereas greater warming is detected in both T_{MIN} and T_{MAX} in the Appalachian Mountains than in its low-lying counterpart.

For other three paired regions, opposite asymmetric warming is observed between each paired regions. The magnitude of the T_{MIN} trend is larger than the T_{MAX} trend on the Northern Tibetan Plateau, whereas the magnitude of the T_{MIN} trend is smaller than that of the T_{MAX} trend in its eastern lower-elevation counterpart (the sampled Loess Plateau). The magnitude of the T_{MIN} trend is smaller than that of the T_{MAX} trend in the East Loess Plateau and the Southeast Rocky Mountains, whereas the T_{MIN} trend is larger than the T_{MAX} trend in their low-lying counterparts (the North China Plain and the eastern low-lying region, respectively). When the regional amplification is estimated for T_{MIN} and T_{MAX} as a whole, the warming is greater on the North Tibetan Plateau than the sampled Loess Plateau (2.26 versus 1.60 °C)and in the

Table 2. Summary of the regional warming trend [Q_{REG}(°C 50-yrs^{-1})], effect coefficients of altitude, latitude and longitude [EC_{ALT}, EC_{LAT}, and EC_{LONG} (°C km^{-1})], and altitudinal amplification trend [Q_{ALTAMP} (°C km^{-1}50-yrs^{-1})] for the high-elevation regions across the globe.

No.	Region	Q_{REG}	EC_{ALT}	EC_{LAT}	EC_{LONG}	Q_{ALTAMP}	n
			Annual mean temperature				
1	Tibetan Plateau	**1.867**	6.0596	0.0091	0.0013	**0.271**	66
2	Loess Plateau	**1.595**	4.8945	0.0045	0.0017	**0.353**	196
3	Yunnan-Guizhou Plateau	**0.779**	3.9007	0.0067	0.0024	**0.148**	183
4	Alps	**1.639**	5.4186	0.0089	0	**0.212**	70
5	United States Rockies	**1.321**	5.7474	0.0060	0	**0.213**	117
6	Appalachian Mountains	**1.754**	5.7996	0.0092	0	**0.180**	42
1a	Northern Tibetan Plateau	**1.955**	6.5443	0.0104	0.0028	**0.176**	38
1b	Southern Tibetan Plateau	**1.847**	5.5027	0.0089	0	**0.522**	28
			Annual mean minimum temperature				
1	Tibetan Plateau	**2.395**	5.7519	0.0101	0.0009	**0.360**	66
2	Loess Plateau	**1.939**	4.9744	0.0068	0.0025	**0.266**	194
3	Yunnan-Guizhou Plateau	**1.251**	4.1371	0.0064	0.0009	**0.329**	180
4	Alps	**1.499**	5.7559	0.0077	0	**0.243**	55
5	United States Rockies	**1.263**	6.6778	0.0055	0	**0.436**	113
6	Appalachian Mountains	**1.945**	4.8559	0.0080	0	**0.202**	41
1a	Northern Tibetan Plateau	**2.420**	6.5421	0.0120	0.0023	**0.193**	38
1b	Southern Tibetan Plateau	**2.495**	5.7618	0.0089	0	**0.697**	28
			Annual mean maximum temperature				
1	Tibetan Plateau	**1.582**	6.1228	0.0089	0.0013	***0.107***	65
2	Loess Plateau	**1.606**	0	0	0	0	196
3	Yunnan-Guizhou Plateau	**0.644**	4.0497	0.0073	0.0059	**0.064**	181
4	Alps	**1.513**	6.2238	0.0036	0	**0.563**	51
5	United States Rockies	**1.547**	0	0	0	0	113
6	Appalachian Mountains	**1.550**	7.1067	0.0100	0	**0.188**	38
1a	Northern Tibetan Plateau	**1.779**	6.5600	0.0099	0.0036	0.068	38
1b	Southern Tibetan Plateau	**1.324**	6.0120	0.0089	0	**0.312**	27

The results for annual mean temperature are cited from Wang et al.[19] with a correction of Q_{ALTAMP} for the US Rockies. Significant trends (at the 0.05 level) are set in bold, with the marginally significant trend (at the 0.10 level) in italic bold.

doi:10.1371/journal.pone.0140213.t002

Southeast Rocky Mountains than its eastern low-lying region (1.54 versus 1.05 °C) during 1961–2010. Greater warming also occurred in the East Loess Plateau than on the North China Plain (1.53 versus 1.42 °C) during the same period.

Discussion

Many factors might have played a role in shaping the patterns of temperature change in high-elevation regions across the globe. However, it is worth noting that these factors might have distinct effects in terms of their magnitudes and directions, and can be defined as basic and non-basic factors in terms of their relative status in the complex interaction hierarchy.

Barry [2] stated that climate in mountain regions is controlled by four basic factors: altitude, latitude, continentality, and topography. A previous study has shown that altitude and latitude are major factors in determining the geographical pattern of temperature change in the Alps [12]. Notably, the effect of energy balance variation on surface temperature was found to be amplified with decreasing temperature in the environment as a result of the functional shape of the Stefan-Boltzmann law [29–30]. Provided that this energy balance effect is a fundamental

Table 3. Same as Table 2 but provided that the temperature change is predominately controlled by two variables (altitude and latitude) rather than three variables (altitude, latitude, and longitude).

No.	Region	EC_{ALT}	EC_{LAT}	Q_{ALTAMP}	n
		Annual mean temperature			
1	Tibetan Plateau	5.6761	0.0095	**0.271**	66
2	Loess Plateau	4.2662	0.0054	**0.341**	196
3	Yunnan-Guizhou Plateau	3.2008	0.0087	**0.148**	183
4	Alps	5.4186	0.0089	**0.212**	70
5	United States Rockies	5.7474	0.0060	**0.213**	117
6	Appalachian Mountains	5.7996	0.0092	**0.180**	42
1a	Northern Tibetan Plateau	5.7606	0.0093	**0.192**	38
1b	Southern Tibetan Plateau	5.5027	0.0089	**0.522**	28
		Annual mean minimum temperature			
1	Tibetan Plateau	5.7519	0.0101	**0.366**	66
2	Loess Plateau	4.0506	0.0080	**0.239**	194
3	Yunnan-Guizhou Plateau	3.8730	0.0071	**0.313**	180
4	Alps	5.7559	0.0077	**0.243**	55
5	United States Rockies	6.6778	0.0055	**0.436**	113
6	Appalachian Mountains	4.8559	0.0080	**0.202**	41
1a	Northern Tibetan Plateau	5.9046	0.0112	**0.202**	38
1b	Southern Tibetan Plateau	5.7618	0.0089	**0.697**	28
		Annual mean maximum temperature			
1	Tibetan Plateau	5.7493	0.0094	**0.112**	65
2	Loess Plateau	0	0	0	196
3	Yunnan-Guizhou Plateau	2.4075	0.0122	**0.067**	181
4	Alps	6.2238	0.0036	**0.563**	51
5	United States Rockies	0	0	0	113
6	Appalachian Mountains	7.1067	0.0100	**0.188**	38
1a	Northern Tibetan Plateau	5.5450	0.0086	0.072	38
1b	Southern Tibetan Plateau	6.0120	0.0089	**0.312**	27

doi:10.1371/journal.pone.0140213.t003

theoretical basis on warming amplification under lower temperature rather than a partial explanation of larger temperature trends in polar and high-altitude climate [29–30], because the higher the altitude (latitude), the lower the temperature [2], the magnitudes of station temperature trends across a high-elevation region will be closely related to both *ALT* and *LAT*. Furthermore, provided that there is a clear temperature gradient with longitude due to continentality, then this will remain true for *LONG* as well. It is based on these observations and deductions that Wang *et al.*[19] have developed the altitudinal warming component extraction equation (AWCE equation).

In fact, a significant negative relationship between T_{AVG} and *ALT*, *LAT* and *LONG* (between T_{AVG} and *ALT* and *LAT*) was detected for three (five) of the eight high-elevation regions tested [19]. A significant altitudinal amplification trend in T_{MEAN} was detected in each region by extracting Q_{ALT} from Q_{TOTAL} at the individual stations in each region using the AWCE equation [19]. Because the same holds good for T_{MIN} and T_{MAX} for the regions where a significant negative relationship exists between T_{AVG} and *ALT*, *LAT* and *LONG* or between T_{AVG} and *ALT* and *LAT*, significant altitudinal amplification trends are detected for T_{MIN} and T_{MAX} in four regions, consistent with the T_{MEAN} results from these regions. In the Loess Plateau and the US Rocky Mountain regions, significant altitudinal amplification trends are detected for T_{MIN},

Table 4. Relationships between station warming rates (Q_{TOTAL}, °C 50-yrs^{-1}) and station altitudes (km) in the high-elevation regions across the globe.

No.	Region	Simple linear regression				n
		r	*p*	$Q_{TOTALAMP}$	*B*	
		Annual mean temperature				
1	Tibetan Plateau	0.027	= 0.830	0.027	1.761	66
2	Loess Plateau	0.280	<0.001	**0.394**	1.175	196
3	Yunnan-Guizhou Plateau	0.287	<0.001	**0.224**	0.502	183
4	Alps	-0.119	= 0.327	-0.062	2.096	70
5	United States Rockies	0.287	= 0.002	**0.229**	0.404	117
6	Appalachian Mountains	0.051	= 0.746	0.070	1.327	42
1a	Northern Tibetan Plateau	-0.079	= 0.635	-0.087	2.252	38
1b	Southern Tibetan Plateau	0.617	<0.001	**0.610**	-0.613	28
		Annual mean minimum temperature				
1	Tibetan Plateau	0.066	= 0.601	0.091	2.090	66
2	Loess Plateau	0.082	= 0.256	0.189	1.840	194
3	Yunnan-Guizhou Plateau	0.299	<0.001	**0.339**	0.837	180
4	Alps	-0.124	= 0.368	-0.163	1.987	55
5	United States Rockies	0.282	= 0.002	**0.344**	0.797	113
6	Appalachian Mountains	-0.027	= 0.865	-0.066	1.734	41
1a	Northern Tibetan Plateau	-0.105	= 0.532	-0.148	2.924	38
1b	Southern Tibetan Plateau	0.468	= 0.012	**0.783**	-0.606	28
		Annual mean maximum temperature				
1	Tibetan Plateau	-0.262	= 0.035	**-0.252**	2.487	65
2	Loess Plateau	0.032	= 0.656	0.047	1.651	196
3	Yunnan-Guizhou Plateau	0.044	= 0.554	-0.085	0.931	181
4	Alps	0.179	= 0.210	0.169	1.755	51
5	United States Rockies	0.108	= 0.256	0.171	1.308	113
6	Appalachian Mountains	0.062	= 0.712	0.120	1.070	38
1a	Northern Tibetan Plateau	-0.334	= 0.040	**-0.332**	2.887	38
1b	Southern Tibetan Plateau	0.331	= 0.091	***0.306***	0.172	27

$Q_{TOTALAMP}$ denotes altitudinal amplification trend of Q_{TOTAL}s, expressed in °C km^{-1}50-yrs^{-1}. *B* represents intercept. Pearson correlation coefficient (*r*) is given with the two-tailed *p* value for each case. Significant trends (at the 0.05 level) are set in bold, with the marginally significant ones (at the 0.10 level) in italic bold. The results for annual mean temperature are cited from Wang et al. [19].

doi:10.1371/journal.pone.0140213.t004

whereas no altitudinal amplification trends are observed for T_{MAX} because no EC_{ALT}, EC_{LAT} and EC_{LONG} are estimated for these two regions due to the small difference in daytime temperatures among the individual stations across both regions.

Quantitatively, the asymmetric altitudinal amplification trends in T_{MIN} and T_{MAX} are consistent with the regional temperature trends in T_{MIN} and T_{MAX} for all the regions, with the exception of the US Rocky Mountains (Table 2). The elevation-dependent warming in minimum temperatures on and around the Tibetan Plateau has been demonstrated by plotting the trends at individual elevation bands versus elevation in the previous studies [11, 14]. In contrast, You et al. [13] failed to substantiate altitudinal amplification trends in most temperature extreme indices derived from daily minimum and maximum temperatures in the eastern and central Tibetan Plateau.

The asymmetric changes in T_{MIN} and T_{MAX} have been reported for a number of large regional series [31–32] and for certain high-elevation regions [15, 33–36]. A stronger warming

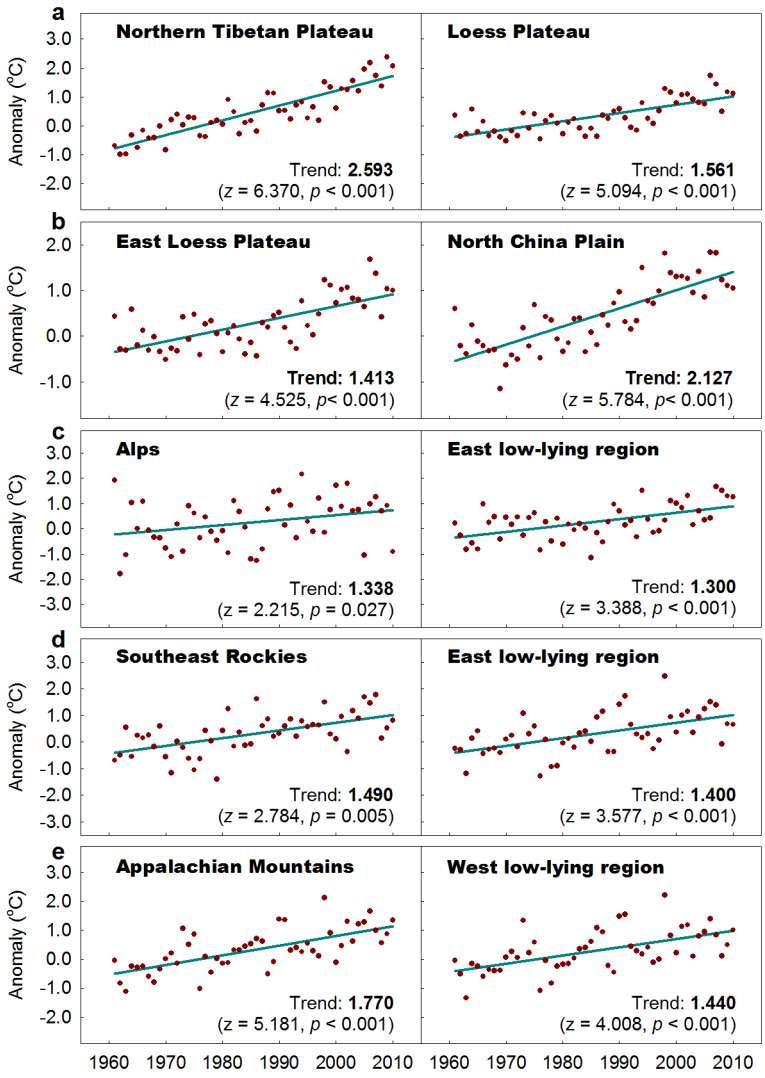

Fig 5. Monotonic trends of annual mean minimum temperature during 1961–2010 over the paired regions shown across the globe. The regional anomaly values are produced by simple averaging of the individual station anomaly values (relative to the 1961 to 1990 means) within each region. The trend is extracted using the Mann-Kendall test method, and expressed in °C 50-yrs^{-1}, with the statistic *z* and its *p* value in parentheses. The significant trend (at the 0.05 level) is set in bold.

doi:10.1371/journal.pone.0140213.g005

for T_{MIN} than T_{MAX} has been observed in the Tibetan Plateau[35–36], the eastern Loess Plateau [37] and the stations located in different elevation ranges in the latitudinal bands 30°N-70°N [34]. Greater warming has been observed in T_{MIN} than T_{MAX} in the Swiss Alps over the period1901–1992[33], whereas similar changes in the minimum and maximum temperatures have been detected in the mountainous regions of Central Europe over the period1901–1990 [17]. The greater warming for T_{MAX} than T_{MIN} observed in this study indicates a shift from stronger warming in T_{MIN} to stronger warming in T_{MAX} for the Alps during 1961–2010. Moreover, McGuire *et al.* [15] found significant warming in T_{MAX} but not in T_{MIN} in the Rocky Mountain Front Range during 1953–2008. The presence of a cooling signal in T_{MIN} along the Front Range [15] and the weaker warming for T_{MIN} than T_{MAX} for the entire US Rocky Mountain region observed in the current study are likely related to changes in regional and local land-use practices [15] and possible changes in atmospheric circulation [38].

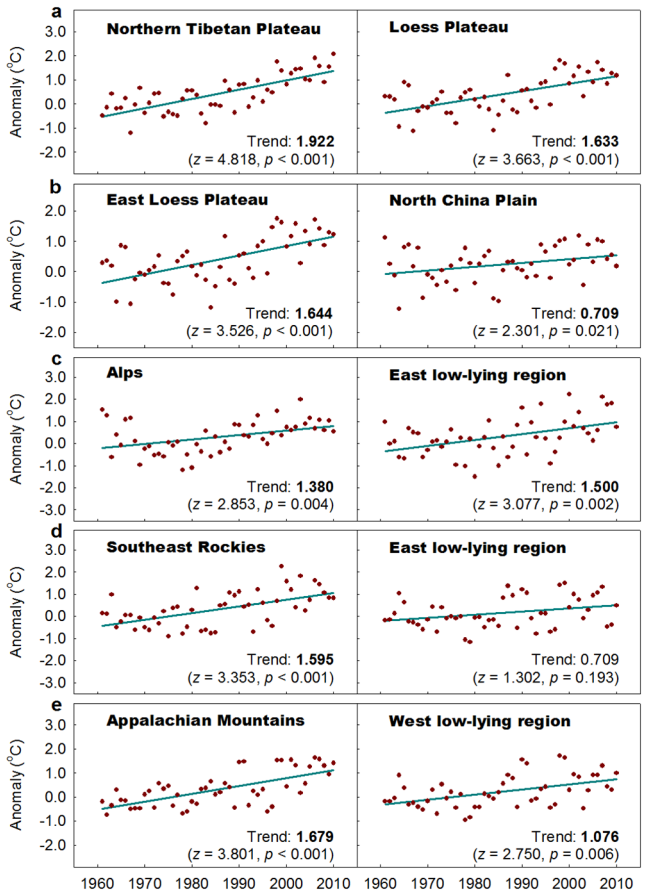

Fig 6. Same as Fig 5 but for annual mean maximum temperature.

doi:10.1371/journal.pone.0140213.g006

In terms of the longitude effect, it is difficult to interpret the meaning of EC_{LONG} except for the above deduction. Nevertheless, similar results are observed for T_{MEAN}, T_{MIN} and T_{MAX} in the high-elevation regions tested (Table 3) when two variables (altitude and latitude) are considered instead of three variables (altitude, latitude and longitude). This indicates that the altitudinal amplification trend in a high-elevation region can be well approximated when these two basic variables are taken into account.

Why is Q_{ALT} so different from Q_{TOTAL} when they are each regressed against *ALT*? First, this is due to Q_{TOTAL}s being predominately controlled by both altitude and latitude over a high-elevation region, while Q_{ALT}s are associated only with altitude, as the name suggests. Consequently, the correlation between Q_{TOTAL} and *ALT* can be reduced by a huge amount of noise, whereas no noise affects the correlation between Q_{ALT} and *ALT*. Relative to the effect (signal) of the target independent variable (*ALT*), the effect of the non-target independent variable (*LAT*), as well as the interacting effect of *LAT* and *ALT*, should be considered noise in the statistical analysis. Second, the magnitude of the noise impact on the correlation between Q_{TOTAL} and *ALT* varies from region to region, depending on the signal intensity (SI) of Q_{TOTAL} in individual regions. According to the SI concept [28], the Q_{TOTAL}SI (signal quantity per unit area) in a region is approximately proportional to the number of available stations in a region and is inversely proportional to the total area of the region. It is probably due to the very high Q_{TOTAL}SI for the Loess Plateau, the Yunnan-Guizhou Plateau, and the US Rockies, but very low Q_{TOTAL} SI for the Tibetan Plateau and the Appalachian Mountains, that a significant

correlation between Q_{TOTAL} and *ALT* is detected for the former, but not for the latter in terms of T_{MEAN} (Table 4). The same holds true for T_{MIN}, excepting that a positive but non-significant correlation between Q_{TOTAL} and *ALT* is observed for the Loess Plateau (Table 4).

Furthermore, the contrasting correlations between Q_{TOTAL} and *ALT* among these regions (particularly between the two sub-regions of the Tibetan Plateau) could be partly attributable to the effect of topography (the underlying feature of the available stations)on them. As revealed in a previous study [19], the underlying topography of the available stations in the Northern Tibetan Plateau (NTP) is characterized by a significant negative ***s***patial ***co***rrelation between the station ***al***titudes and station ***la***titudes (*SCOALLA*), whereas no significant negative *SCOALLA* occurs in the Southern Tibetan Plateau (STP); indicating that the altitude effect could be cancelled out (or overwhelmed) by the latitude effect in the NTP while not in the STP [19]. Therefore, the correlation between Q_{TOTAL} and *ALT* is non-significant (negatively significant) for T_{MEAN} and T_{MIN} (T_{MAX}) over the NTP, while the correlation between Q_{TOTAL} and *ALT* is positively significant (marginally significant) for T_{MEAN} and T_{MIN} (T_{MAX}) over the STP (Table 4). Owing to that, the correlation between Q_{TOTAL} and *ALT* for the entire Tibetan Plateau is a reflection of those two sub-regions, and the number of stations from the NTP is obviously larger than that from the STP, the correlation between Q_{TOTAL} and *ALT* for the entire Tibetan Plateau is closer to that of the NTP rather than the STP (Table 4).

In addition, it should be noted that although the negative *SCOALLA* has no direct influence on the correlation between Q_{ALT} and *ALT*, it may more or less affect the long-term average values of T_{MEAN}, T_{MIN} and T_{MAX}, and consequently the EC_{ALT} and EC_{LAT}. This, in turn, could have affected the magnitudes of Q_{ALT}s, and therefore the relationship between Q_{ALT} and *ALT*. It is probably due to this indirect influence that the magnitudes of altitudinal amplification trends appear underestimated for the Tibetan Plateau and the Northern Tibetan Plateau relative to the Southern Tibetan Plateau (Table 2). However, the topographical effect is difficult to quantify, and this effect can only be taken as noise relative to the direct effects of altitude and latitude. Hence it is not taken into account in the quantitative estimation of Q_{ALT}s.

For comparative purpose, the global base EC_{ALT} and EC_{LAT} were also estimated for T_{MIN} and T_{MAX}. The base EC_{ALT} and EC_{LAT} were computed according to the data from all the high ($\geq$200 m above sea level) and low ($<$200 m above sea level) elevation stations, respectively, for either index using the same method as for T_{MEAN} [19]. The result shows that the global base EC_{ALT} values in T_{MEAN}, T_{MIN} and T_{MAX}(4.9±0.9, 5.0±1.2and 3.1±2.8 °C km^{-1}, respectively) are smaller than the average EC_{ALT} values in T_{MEAN}, T_{MIN} and T_{MAX} (5.3±0.8, 5.4±0.9 and 3.9±3.2 °C km^{-1}, respectively) for the six high-elevation regions, and the global base EC_{LAT} values in T_{MEAN}, T_{MIN} and T_{MAX}(0.0049±0.0037, 0.0045 ±0.0028, and 0.0048 ±0.0036 °C km^{-1}, respectively) are clearly smaller than the average EC_{LAT} values in T_{MEAN}, T_{MIN} and T_{MAX} (0.0074 ±0.0020, 0.0074±0.0016, and 0.0050±0.0044 °Ckm^{-1}, respectively) for these regions. This suggests that there exists not only an enhanced EC_{ALT} but also an enhanced EC_{LAT} in the high-elevation regions. Therefore, a greater warming usually occurs in high-elevation regions relative to their lower elevation counterparts.

The slightly greater warming in T_{MIN} and even weaker warming in T_{MAX} in the Alps relative to its low-lying counterpart are likely associated with the greater urban heat effect in the low-elevation area because the urban heat effect is generally greater at low-elevation sites [9, 17]. On the other hand, the unusually stronger warming in T_{MIN} relative to T_{MAX} over the North China Plain could have partially resulted from the unusually large urban heat effect on T_{MIN} relative to T_{MAX}. The urban heat effect is primarily a nocturnal phenomenon in certain places around the world [39–40]. The North China Plain may be one such place. The large difference between changes in T_{MIN} and T_{MAX} between the East Loess Plateau and the North China Plain is also likely related to the barrier effect of the Taihang Mountains, which run from north to

south in North China, forming a natural boundary between the paired regions and a physical barrier to the southeast summer monsoon in China. In fact, the trends in various precipitation indices also differ between the East Loess Plateau and the North China Plain due to this barrier effect. For instance, Fan *et al*. [37] observed a significant decreasing trend (-15.05mm 50-yrs^{-1}) in annual total precipitation on wet days (PRCPTOT) over the entire Shanxi Province, whereas a non-significant trend was observed in PRCPTOT over the northern half of the North China Plain. These two regions are nearly equivalent to the East Loess Plateau and North China Plain in this study.

Considerable seasonal variations in trend magnitude have been observed [11, 14, 30, 38]. The warming amplifications in high-elevation regions may vary greatly on sub-annual scales due to changes in atmospheric circulation and local processes, such as snow albedo and water vapor feedbacks [38, 41]. An improved understanding of altitudinal amplification on sub-annual scales may have more important bearings on societal, ecological and physical systems in high-elevation regions. Therefore it is of great important to characterize the seasonal and monthly pictures of warming amplification of T_{MEAN}, T_{MIN} and T_{MAX} on a global scale.

Conclusions

In this study, analysis of T_{MIN} and T_{MAX} series (1961–2010) show a significant altitudinal amplification trend in T_{MIN} (T_{MAX}) in six (four) of the high-elevation regions tested. The average magnitude of altitudinal amplification trends for the six high-elevation regions is substantially larger (smaller) for T_{MIN} (T_{MAX}) [0.306±0.086 °C km^{-1}(0.154±0.213 °C km^{-1})] than T_{MEAN} (0.230±0.073 °C km^{-1}) in the period 1961–2010. Similar results are obtained when the effects of two variables (altitude and latitude) are considered instead of three variables (altitude, latitude and longitude). For the five paired high- and low-elevation regions available, regional amplification is detected in four high-elevation regions for T_{MIN} and T_{MAX} (respectively or as a whole), whereas it is only observed for T_{MIN} in the fifth high-elevation region. Qualitatively, highly (largely) consistent results are observed for T_{MIN} (T_{MAX}) compared with those for T_{MEAN}. The results for T_{MIN} (T_{MAX}) are basically in conformity with our expectations. These results confirm the effectiveness of the AWCE equation in quantifying altitudinal amplification trend within a high-elevation region. Future study is required to explore the seasonal and monthly patterns of warming amplification trends in T_{MEAN}, T_{MIN} and T_{MAX} on a global scale.

Acknowledgments

We are very thankful to Dr. Roger Gifford (CSIRO) for insightful comments on the manuscript.

Author Contributions

Conceived and designed the experiments: XF QW MW. Performed the experiments: XF QW MW. Analyzed the data: XF QW MW CVJ. Contributed reagents/materials/analysis tools: XF QW CVJ. Wrote the paper: XF QW MW CVJ.

References

1. Barry RG. Changes in mountain climate and glacio-hydrological responses. Mt Res Dev. 1990; 10: 161–170.
2. Barry RG. Mountain climatology and past and potential future climatic changes in mountain regions: a review. Mt Res Dev. 1992; 12(1): 71–86.
3. Barry RG. Recent advances in mountain climate research. Theor Appl Climatol. 2012; 110: 549–553.

4. Rangwala I, Miller JR. Climate change in mountains: a review of elevation-dependent warming and its possible causes. Climatic Change. 2012; 114: 527–547.
5. Mountain Research Initiative EDW Working Group. Elevation-Dependent Warming in Mountain Regions of the World. Nature Clim Change. 2015; 5: 424–430.
6. Liu X, Chen B. Climate warming in the Tibetan Plateau during recent decades. Int J Climatol. 2000; 20: 1729–1742.
7. Vuille M, Bradley RS. Mean annual temperature trends and their vertical structure in the topical Andes. Geophys Res Lett. 2000; 27: 3885–3888.
8. Vuille M, Bradley RS, Werner M, Keimig F. 20th century climate change in the tropical Andes: Observations and model results. Climatic Change. 2003; 59: 75–99.
9. Pepin NC, Lundquist JD. Temperature trends at high elevations: patterns across the globe. Geophys Res Lett. 2008; 35: L14701.
10. You Q, Kang S, Pepin N, Flügel W, Yan Y, Behrawan H, et.al. Relationship between temperature trend magnitude, elevation and mean temperature in the Tibetan Plateau from homogenized surface stations and reanalysis data. Global Planet Change. 2010; 71: 124–133.
11. Yan L, Liu X. Has climatic warming over the Tibetan Plateau paused or continued in recent years? J Earth Ocean Atmos Sci. 2014; 1, 13–28.
12. Beniston M, Rebetez M. Regional behavior of minimum temperatures in Switzerland for the period 1979–1993. Theor Appl Climato. 1996; 53: 231–243.
13. You Q, Kang S, Pepin N, Yan Y. Relationship between trends in temperature extremes and elevation in the eastern and central Tibetan Plateau, 1961–2005. Geophys Res Lett. 2008; 35:L14704.
14. Liu X, Cheng Z, Yan L, Yin Z. Elevation dependency of recent and future minimum surface air temperature trends in the Tibetan Plateau and its surroundings.Global Planet Change. 2009; 68:164–174.
15. McGuire CR, Nufio CR, Bowers MD, Guralnick RP. Elevation-dependent temperature trends in the Rocky Mountain Front Range: changes over a 56-and 20-year record. PloS ONE. 2012; 7, e44370. doi: 10.1371/journal.pone.0044370 PMID: 22970205
16. Falvey M, Garreaud RD. Regional cooling in a warming world: Recent temperature trends in the southeast Pacific and along the west coast of subtropical South America (1979–2006). J Geophys Res. 2009; 114: D04102.
17. Weber RO, Talkner P, Auer I, Bohm R, Gajic-Capka M, Zaninovic K, et al. 20th-century changes of temperatures in the mountain regions of Central Europe. Climatic Change. 1997; 36, 327–344.
18. Jungo P, Beniston M. Changes in the anomalies of extreme temperature anomalies in the 20th century at Swiss climatological stations located at different latitudes and altitudes. Theor Appl Climatol. 2001; 69, 1–12.
19. Wang Q, Fan X, Wang M. Recent warming amplification over high elevation regions across the globe. Clim Dynam. 2014; 43, 87–101.
20. Lawrimore JH, Menne MJ, Gleason BE, Williams CN, Wuertz DB, Vose RS, et al. An overview of the Global Historical Climatology Network monthly mean temperature data set, version 3. J Geophys Res. 2011; 116: D19121.
21. Martinez R, Nieto JJ, Freire A, van den Besselaar EJM, Klein Tank AMG, van der Schrier G. Daily dataset for climate extreme analyses in Latin America [Internet]. Latin American Climate Assessment and dataset. 2012. Available: http://lacad.ciifen.org.
22. Klein Tank AMG, Wijngaard JB, Können GP, Böhm R, Demarée G, Gocheva A, et al. Daily dataset of 20th-century surface air temperature and precipitation series for the European Climate Assessment. Int J Climatol. 2002; 22: 1441–1453.
23. Wang XL, Feng Y. RHtestsV3 User Manual [Internet]. ETCCDI/CRD Climate Change Indices. 2010. Available: http://cccma.seos.uvic.ca/ETCCDMI/RHtest/RHtestsV3_UserManual.doc
24. Mann HB. Nonparametric tests against trend. Econometrika. 1945; 13: 245–259.
25. Kendall MG. Rank Correlation Methods. 4th ed. London: Charles Griffin; 1975.
26. Sen PK. Estimates of the regression coefficient based on Kendall's tau. J Am Stat Assoc. 1968: 63: 1379–1389.
27. Wang XL, Swail VR. Changes of extreme wave heights in Northern Hemisphere oceans and related atmospheric circulation regimes. J Climate. 2001; 14: 2204–2220.
28. Wang Q, Fan X, Wang M. Evidence of high-elevation amplification versus Arctic amplification. Sci Rep. 2015; In press.
29. Ohmura A. On the cause of "Fram" type seasonal change in diurnal amplitude of air temperature in polar regions. J Climatol. 1984; 4:325–338.

30. Ohmura A. Enhanced temperature variability in high-altitude climate change. Theor Appl Climatol.2012; 110: 499–508.

31. Easterling DR. Recent changes in frost days and the frost-free season in the United States. B Am Meteorol Soc. 2002; 83: 1327–1332.

32. Easterling DR, Horton B, Jones PD, Peterson TC, Karl TR, Parker DE,et al. Maximum and minimum temperature trends for the globe. Science. 1997; 277: 364–367.

33. Beniston M, Rebetez M, Giorgi F, Marinucci MR. An analysis of regional climate change in Switzerland. Theor Appl Climatol. 1994; 49: 135–159.

34. Diaz HF, Bradley RS. Temperature variations during the last century at high elevation sites. Climatic Change. 1997; 36, 253–279.

35. Duan A, Wu G, Zhang Q, Liu Y. New proofs of the recent climate warming over the Tibetan Plateau as a result of the increasing greenhouse gases emissions. Chinese Sci Bull. 2006; 51:1396–1400.

36. Liu X, Yin Z-Y, Shao X, Qin N. Temporal trends and variability of daily maximum and minimum, extreme temperature events, and growing season length over the eastern and central Tibetan Plateau during 1961–2003. J Geophys Res. 2006; 111, D19109.

37. Fan XH, Wang QX, Wang MB. Changes in temperature and precipitation extremes during 1959–2008 in Shanxi, China.Theor Appl Climatol. 2012; 109: 283–303.

38. Ceppi P, Scherrer S, Fischer A, Appenzeller C. Revisiting Swiss temperature trends 1959–2008. Int J Climatol. 2010; 32(2): 203–213.

39. Jauregui E. Possible impact of urbanization on the thermal climate of some large cities in Mexico. Atmosfera. 2005; 18: 249–252.

40. Si P, Ren Y, Liang DP, Lin BW. The combined influence of background climate and urbanization on the regional warming in Southeast China. J Geographical Sci. 2012; 22: 245–260.

41. Rangwala I. Amplified water vapour feedback at high altitudes during winter. Int J Climatol. 2013; 33 (4): 897–903.